SAND76-0074
Unlimited Release

Determination of the Solid-Liquid-Vapor Triple Point Pressure of Carbon

David M. Haaland

Prepared by Sandia Laboratories, Albuquerque, New Mexico 87115 and Livermore, California 94550 for the United States Energy Research and Development Administration under Contract AT(29–1)-789

Printed January 1976

Sandia Laboratories

SF 2900 Q(7-73)

When printing a copy of any digitized SAND Report, you are required to update the markings to current standards.

Issued by Sandia Laboratories, operated for the United States Energy Research and Development Administration by Sandia Corporation.

NOTICE

This report was prepared as an account of work sponsored by the United States Government. Neither the United States nor the United States Energy Research and Development Administration, nor any of their employees, nor any of their contractors, subcontractors, or their employees, makes any warranty, express or implied, or assumes any legal liability or responsibility for the accuracy, completeness or usefulness of any information, apparatus, product or process disclosed, or represents that its use would not infringe privately owned rights.

Printed in the United States of America
Available from
National Technical Information Service
U. S. Department of Commerce
5285 Port Royal Road
Springfield, VA 22151
Price: Printed Copy $5.00
Microfiche $2.25

SAND 76-0074
Unlimited Release

DETERMINATION OF THE SOLID-LIQUID-VAPOR TRIPLE POINT PRESSURE OF CARBON*†

January 1976

David M. Haaland
Division 5825
Sandia Laboratories
Albuquerque, NM 87115

ABSTRACT

A detailed experimental study of the triple point pressure of carbon using laser heating techniques has been completed. Uncertainties and conflicts in previous investigations have been addressed and substantial data presented which places the solid-liquid-vapor carbon triple point at 107 ± 2 atmospheres (10.8 ± 0.2 MPa). This is in agreement with most investigations which have located the triple point pressure between 100 and 120 atmospheres (10 to 12 MPa), but is in disagreement with recent low pressure carbon experiments. The absence of any significant polymorphs of carbon other than graphite suggests that the graphite-liquid-vapor triple point has been measured.

Graphite samples were melted in a pressure vessel using a 400 W Nd:YAG continuous-wave laser focused to a maximum power density of ~ 80 KW/cm^2. Melt was confirmed by detailed microstructure analysis and x-ray diffraction of the recrystallized graphite. Experiments to determine the minimum melt pressure of carbon were completed as a function of sample size, type of inert gas, and laser power density to assure that: 1) laser power densities were sufficient to produce melt at the triple point pressure of carbon and 2) the pressure of carbon at the surface of the sample was identical to the measured pressure of the inert gas in the pressure vessel.

High-speed color cinematography of the carbon heating revealed the presence of a laser-generated vapor or particle plume in front of the sample. The existence of this bright plume prevented the measurement of the carbon triple point temperature.

*This work was supported by the U.S. Energy Research & Development Admin.

†Portions of this work were presented at the 12th Biennial Conf. on Carbon, U.of Pittsburgh,PA, 28 Jul-1 Aug, 1975 and appeared in the 12th Biennial Conference on Carbon, Extended Abstracts and Program, p. 51.

CONTENTS

		Page
I.	Introduction	9
II.	Experimental Apparatus and Procedures	14
III.	Results and Discussion	20
	Confirmation of Melt	20
	Laser Irradiation and Temperature Measurements	23
	Triple Point Pressure	27
	Polymorphs of Carbon	33
IV.	Conclusions	34
	Appendix A	35
	Appendix B	39
	Appendix C	42
	References	44
	Acknowledgments	48

FIGURES

Figure		Page
1	Diagram of pressure vessel used in carbon melting experiments.	15
2	Schematic diagram of experimental apparatus.	16
3	Laser cratered rod of pyrolytic graphite showing droplet of recrystallized melt at the bottom of the crater (147 atm Ar).	21
4	Microstructure of recrystallized melt at the bottom of the crater. The growth cones of the original pyrolytic graphite are evident underneath the droplet (147 atm Ar).	21
5	Microstructure of pyrolytic graphite heated with the laser at maximum power density but below the carbon triple point (105 atm Ar).	22
6	X-ray powder diffraction patterns of the original pyrolytic graphite samples (top), vapor deposits of carbon surrounding the crater of a laser heated sample (middle), and recrystallized melt from the bottom of the crater (bottom).	24
7	Representative pyrometer output as a function of time. Note that pyrometer output is non-linear with temperature and is not sensitive to temperatures below 2500K. Temperatures are brightness temperatures corrected for fused silica windows. Sample was 1.5 mm diameter pyrolytic graphite in 147 atm argon irradiated at ~ 35 KW/cm^2.	26

TABLES

Table		Page
I	Triple Point Data For Carbon	10
II	Impurities Present in HPG Pyrolytic Graphite	17
III	Results of Carbon Melting Experiments	28
IV	Results of Carbon Melting Experiments	29

I. Introduction

The triple point of carbon has received considerable attention throughout this century with controversy often surrounding the subject. Before the work of Bassett[1,2] in 1939, the debate focused on whether carbon melted or sublimed at atmospheric pressure. Bassett made the first effort to quantitatively determine the triple point pressure of carbon. His data led him to conclude that a pressure of ~ 102 atm (~ 10.3MPa) was required before carbon would melt. After the publication of these results, more than half a dozen additional investigations[3-12] have also resulted in the conclusion that the triple point pressure of carbon was between 100 and 120 atm (10 and 12 MPa) with the triple point temperature determinations ranging between 3670 K and 4300 K.* (These results and others are given in detail in Appendix A and summarized in Table I.) However, theoretical calculations based on extrapolated carbon vapor pressures and thermodynamic functions have indicated that the vapor pressure of carbon does not reach 100 atm (10 MPa) until temperatures of 4570-5200 K are achieved.[13-15] The most recent estimate is 4765 K.[14] Clearly, the theoretical predictions and experimental values are not in agreement. Recently, Whittaker et al.[16,17] offered a possible resolution of this conflict by presenting controversial evidence that the carbon triple point pressure was less than one atmosphere.

In addition to the general lack of experimental precision and the conflicts between experiment and theory, a number of difficulties and uncertainties persist with the previous data. A major assumption that has been made in the past carbon triple point work is that the vapor pressure of carbon is equal to the pressure of the gas used to pressurize the system. This is required since it is the pressure of carbon vapor at the surface that defines the triple point pressure, not the pressure of the inert gas in the chamber. Thus it has generally

---

*Fateeva et al.[7] originally reported a carbon triple point temperature of 4650 K. Later they corrected their value to 4040 K,[9] stating that the earlier temperature was in error due to improper pyrometer filter correction.

TABLE I. TRIPLE POINT DATA FOR CARBON

Investigator	(Year)	Heating Method	Pressurizing Gas	Pressure (atm)	Temp (K)
Bassett[1,2]	1939	Resistive	Ar	102	4000
Steinle[3]	1940	Resistive	Ar, N_2	100	3670
Jones[4]	1958	Resistive	Ar	100	3840
Noda[5,6]	1959	Resistive	Ar	110-120	4020
Fateeva et al.[7]	1963	Resistive	Ar	100 ± 10	4650
Fateeva et al.[9]	1969	Resistive	Ar	100	4040
Schoessow[10]	1967	Resistive	He	103	4180-4300
Diaconis et al.[11]	1971	Resistive & Arc Image	Ar, N_2	102	4100-4300
Gokcen[12]	1976	HF Laser	Ar, Ne, Kr	120 ± 10	4130
Whittaker & Kintner[17]	1975	CO_2 Laser	Ar	0.19	3870
Haaland (this work)	1975	Nd:YAG Laser	Ar, He	107 ± 2	----

Theoretical		Method	Assumed Pressure (atm)	Calculated Temperature (K)
JANAF[15]	1961	Extrapolated Total Vapor Pressure	100	5200
Palmer & Shelef[13]	1968	Vapor Pressure Data Analysis	100	4570
Leider et al.[14]	1973	New Thermal Furnctions, Heats of Formation, New Vapor Pressure Analysis	103	4765

been assumed, but not previously confirmed, that the minimum melt pressure determined from the inert gas pressure is identical to the triple point pressure of carbon. For the carbon vapor pressure to be equal to the gas pressure, the rate of vaporization must exceed the transport of carbon away from the sample surface. If this is not the case, then the measured minimum pressure for melt is only an upper limit for the triple point pressure. Considerable effort was made in this work to confirm that the carbon vapor pressure was identical to the pressure of the inert gas.

Another point of concern with some of the previous investigations is the method of determining whether melting had occurred. All investigators have used the observation of the sample after it had cooled to prove the presence of melt. Most of these involved only a visual observation of the sample surface. However, Steinle[3] has shown that vapor deposited carbon can exhibit flow patterns and external appearances that are generally characteristic of resolidified melt. Therefore, surface examination of the samples can lead to ambiguous results. Schoessow[10] did section his samples and view them with optical microscopy but gives no information about the microstructure observed nor did he use the microstructure as a criterion for confirming recrystallized melt. Dianconis et al.[11] present the only details regarding the detailed microstructure of the recrystallized melt. Using polarized-light microscopy to achieve greater structural detail and contrast in sectioned and polished samples, Diaconis et al. were able to easily distinguish between recrystallized melt and vapor deposited carbon. The recrystallized material was a low density structure of large, randomly oriented graphite crystallites. The vapor deposited material was distinguished as a very fine crystalline material characteristic of nucleation and condensation from a vapor. Several investigators[3,5,6,18] have also completed x-ray analysis of the recrystallized melt and observe a sharpening of the diffraction lines and a reduction in d-spacing implying larger and more ordered crystallites than present in the original carbon or the vapor deposited material. Although the narrowing of the diffraction lines appears to be a

necessary condition for confirming melt, apparently it is not a sufficient condition since stress-annealed pyrolytic graphite exhibits the same sharp diffraction without being taken through the liquid phase.[19]

Other uncertainties may arise from the use of resistance heating to achieve carbon melt. Margrave[20] points out that the heats of sublimation of carbon ions (C_n^-) are smaller in absolute magnitude than those of the corresponding neutral carbon species (C_n). Thus resistive heating, which supplies a large number of electrons, could result in C_n^- (rather than C_n) becoming significant equilibrium vapor species at high temperatures. Margrave suggests that laser heating be used to resolve this problem. Laser heating also has the advantage that energy is supplied to the surface of the sample. Steady-state resistive heating tends to heat carbon internally with the possibility of producing additional pressure gradients because of the greater thermal expansion within the interior of the sample.

Further uncertainties in previous triple point work arise from the absence of detail presented concerning the pressure measurement methods or their accuracy. It appears that there has been a general lack of attention paid to accurately determining carbon triple point pressure. Naturally, after the work of Bassett, most efforts were centered on temperature rather than pressure. To facilitate temperature measurements, large samples and small pressure vessel volumes were used. Thus large pressure excursions were experienced during the heating cycle. Jones[4] reports a factor of two increase in pressure during his carbon melting experiments whereas no mention of the magnitude of pressure increase is made by other investigators. Even in the few cases where pressure was continuously monitored, the accuracy of determining minimum melt pressure with this situation is greatly decreased if pressure increases are significant. By keeping the pressure rise small, the triple point pressure error range can be narrowed considerably.

The previous triple point pressure measurements also suffer in that there has been no effort made to confirm that sufficient power is deposited in the sample to assure that the minimum melt pressure is not power limited. Because the vaporization rate of carbon increases

as the external gas pressure decreases, significant additional vaporization heat loses can occur if the applied pressure is decreased. If sufficient power is not supplied to the sample, abnormally high pressures may be required to melt the carbon. Under these conditions, the experimentally determined minimum melt pressure would only be an upper limit to the triple point pressure and would be a function of power deposition.

Finally, a number of errors or uncertainties can and do arise in experimentally measuring the temperature. Emissivity corrections in this temperature range are in dispute for carbon.[21-24] It has been suggested[24] that particle emission from hot graphite can influence emissivity as well as obscure the surface of the heated sample. Using a simulated black-body cavity, Schoessow[10] eliminated some, but not all of these problems as discussed in Appendix A. Carbon vapor and dense convection currents can also effect temperatures by preventing a clear optical path. The above problems have tended to put a lower limit on the measured temperatures.

The research presented in this paper was initiated to resolve these problems and uncertainties and to better define the triple point of carbon.

II. Experimental Apparatus and Procedures

The pressure vessel used (Fig. 1) was a modified one-liter Autoclave Engineers' vessel with 3 fused silica windows placed along a horizontal circumference of the vessel body at the level of the sample and spaced at 45° intervals. This arrangement permitted simultaneous normal laser heating, optical pyrometry at 45°, and high-speed color cinematography at 90°. Fig. 2 presents a schematic diagram of the apparatus. The silica pressure windows were shielded from carbon deposition by fused silica slides placed between the sample and windows. These slides prevented damage to the laser window and facilitated window cleaning and maintenance. Matheson prepurified grade argon (99.998% min.) or Matheson ultra high purity helium (99.999% min.) were used to pressurize the vessel in all melt experiments.

The carbon samples were rods of graphite 12 mm long and 0.75 mm to 2.5 mm in diameter. Each rod was suspended vertically in the pressure vessel with the laser beam irradiating the rod perpendicular to its axis. Samples of Union Carbide HPG pyrolytic graphite, Union Carbide SPK spectroscopic graphite electrodes, and Poco grade AXF-Q1 graphite were used. The vessel was constructed so that the samples could be raised, lowered or rotated while in place. The pyrolytic graphite rods were machined such that the axis of the rods was the c-axis of the pyrolytic graphite. By irradiating only the edges of the basal planes with the laser, heating was confined to a narrow disc on the rod due to the low thermal conductivity along the c-axis. Thus radiative and conductive heat losses were held to a minimum for these samples. The impurity levels for the HPG material as determined by emission spectroscopy are given in Table II.

Heating of the carbon samples was accomplished with a Holobeam (model 2500-4 R) 400 watt Nd:YAG continuous-wave laser (1.06 μm wavelength) focused by means of 100 mm or 150 mm focal length lenses onto the lower portion of the graphite rod. Power densities were approximated by assuming that the crater dimension along the c-axis was representative of the laser spot diameter. It was also assumed that the power distribution across the spot was uniform rather than gausian

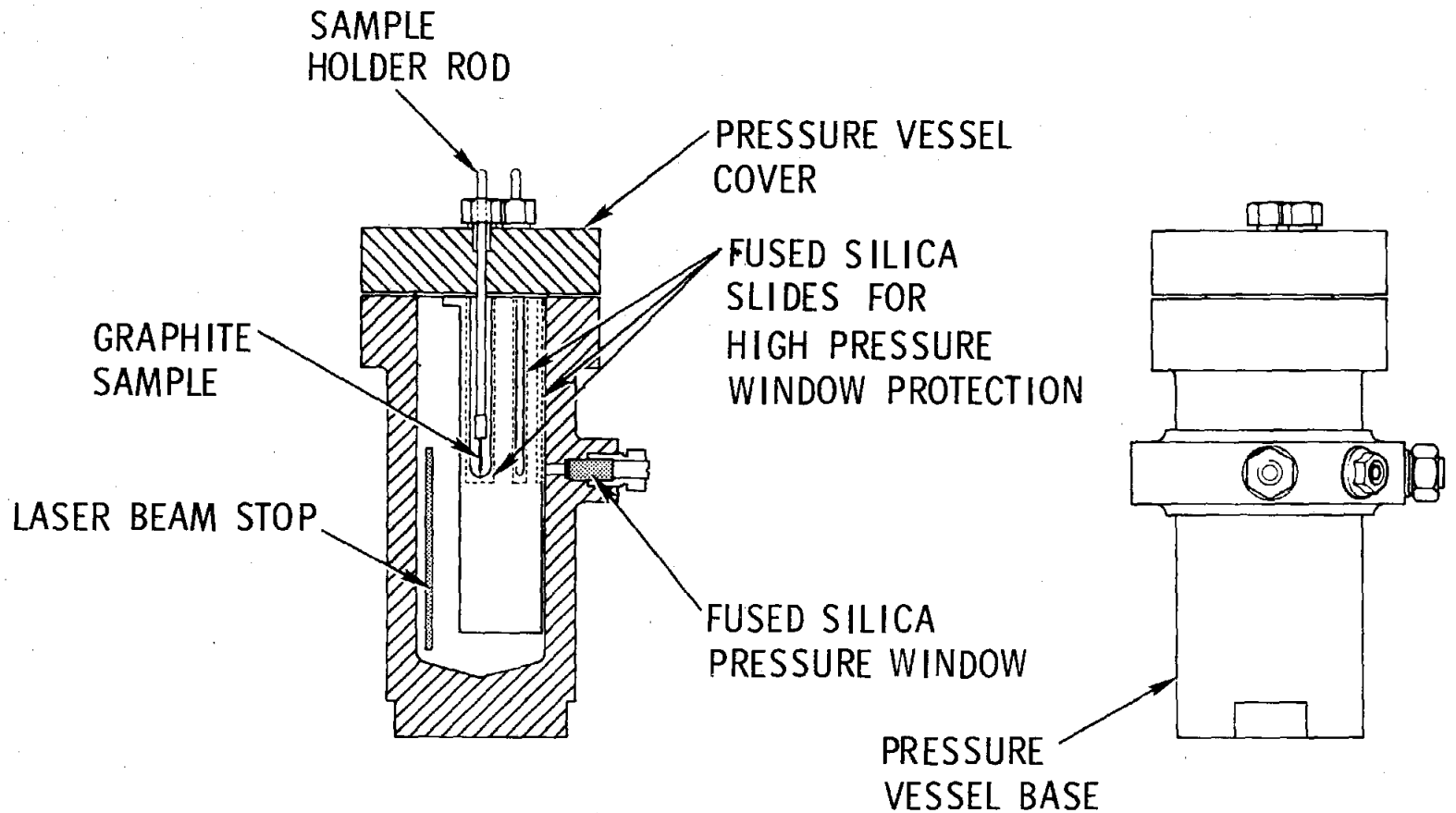

FIGURE 1. DIAGRAM OF PRESSURE VESSEL USED IN CARBON MELTING EXPERIMENTS.

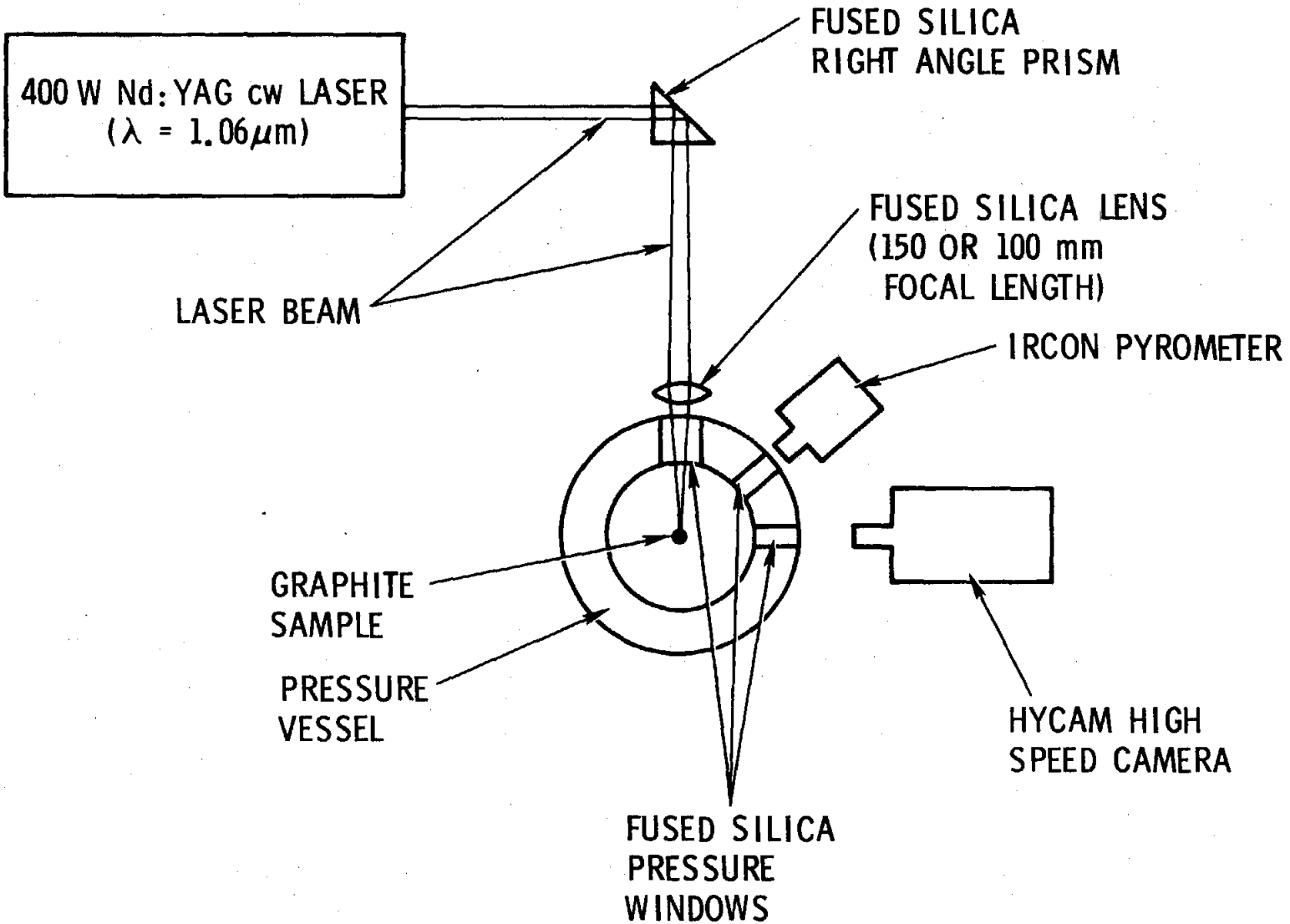

SCHEMATIC DIAGRAM OF EXPERIMENTAL APPARATUS

FIGURE 2. SCHEMATIC DIAGRAM OF EXPERIMENTAL APPARATUS.

TABLE II

IMPURITIES PRESENT IN HPG PYROLYTIC GRAPHITE

Impurity	ppm-wt
B	.02
Fe	.2-2
Si	3
Cu	1
Ca	1
Al	1
H	<5

since the laser was operated in a multi-mode configuration. Both these assumptions tend to minimize the maximum laser power density calculated. Operating at the maximum laser power of 400 W, the calculated maximum power densities achieved were ~ 80 KW/cm^2 and ~ 35 KW/cm^2 with the 100 and 150 mm lenses respectively. Lasing time was controlled automatically with an Industrial Timer Corp. type A tandem recycling timer. Laser power was monitored with a Coherence model no. 213 calorimeter with a $\pm$ 5% accuracy. The laser power could be decreased without changing beam divergence with the introduction of an Isomet TeO_2 acoustic-optic beam modulator.[25]

The temperature was continuously measured during the heating cycle with an Ircon Modline 2000 series pyrometer with a 0.01 second response time and a wavelength sensitivity range of 0.7-0.9 μm. A special 0.98 μm cut-off filter was used to prevent interference from reflected laser radiation. Because of the small $\frac{1}{4}$ inch (0.65 cm) diameter aperture of the fused silica window, the pyrometer was fitted with an internal aperture to prevent the small window from limiting the field of view. Calibration of the pyrometer was made with and without the aperture using a Thermogauge double entry graphite tube furnace as a black-body source and calibrating the Ircon against a model 8640 Leeds and Northrup automatic optical pyrometer. The effective emissivity (A-factor) of the aperture was determined and found to be constant within experimental error. The pyrometer was focused at the level of laser irradiation to a spot size which was $\sim 1/3$ to $1/2$ the rod diameter. Its output was then recorded on a fast response Hewlett-Packard 7402 A strip-chart recorder.

High-speed motion pictures of the heating event were taken with a Hycam camera operated at ~ 1000 frames (with a frame exposure time of 0.4 ms). The film used was Kodak 16 mm Ectachrome EF in 100 ft. rolls. Oriel neutral density filters were often used to obtain proper exposure intensity.

Pressure was continually monitored to within 0.3% with a Teledyne Taber 2101 pressure transducer. Because the volume of the pressure vessel was large and the sample size small, the pressure rise during

the carbon heating was only 0.2 - 1.0 atm (0.02 - 0.1 MPa) depending upon laser heating time. The output of the transducer was also recorded on the Hewlett-Packard 7402A strip chart recorder.

After placing the sample in the pressure vessel and aligning it in the focal spot of the focused laser beam, the vessel was evacuated and backfilled to several atmospheres with inert gas. To eliminate traces of residual air, this gas was then pumped out to a chamber pressure of $<10\ \mu$ and the vessel filled with inert gas to the desired pressure. The laser was fired for the time required to crater 60-90% through the sample so that the measured temperature either reached a maximum or constant value. The laser was focused $\sim$ 1 mm from the bottom of the sample to minimize the conduction of heat down the rod. The chamber pressure and sample temperature were continuously monitored during each experiment.

Frequently the heating event was recorded with high-speed cinematography at 45° or 90° to the incident laser beam. After irradiation, the sample was removed and viewed under an optical microscope for evidence of melt. To confirm melt, the samples were often potted, sectioned, polished and viewed under polarized light to obtain the detailed microstructure of the material. In addition, samples were selected for x-ray and electron diffraction to monitor changes in structure and to search for the presence of carbon polymorphs.

Because pressure excursions during heating were as great as 1.0 atm (0.1 MPa), the minimum melt pressures were determined by lowering the pressure in 2 atm steps. This would place the accuracy of these determinations at ± 2 atm (± 0.2 MPa) even though the pressures were measured and reproduced accurately to 0.3 atm (0.03 MPa).

III. Results and Discussion

Confirmation of Melt. Because only 400 watts of laser power were available, several experimental parameters (sample size, inert gas, chamber pressure, and laser power density) were varied until the input power sufficiently exceeded the heat loses so that carbon melt could be achieved. The first visible detection of melt was the presence of a small recrystallized droplet in the bottom of the laser-created crater. A photograph of a typical droplet produced in a pyrolytic graphite sample is presented in Fig. 3. Soot deposits have been carefully removed from the surface of the droplet to reveal a recrystallized melt which has a highly reflecting surface very similar to that of stress-annealed pyrolytic graphite. Selected samples were potted, sectioned, polished, and photographed under polarized light. As exhibited in Fig. 4, the microstructure is typical of solidification on a surface. Adjacent to the unmelted surface, densely packed graphite crystals grew into the melt. The remainder of the recrystallized melt is a loose, randomly oriented structure of crystallites which were apparently individually nucleated and grew until they impinged on neighboring crystallites. Identical microstructure characteristics were found by Diaconis et al.[11] in their resistive and arc melted graphites. The low density of crystallites in the outer portion of the droplet would indicate that the melt underwent significant contraction upon cooling. The microstructure of those samples which were heated and contained no external traces of droplets were examined (Fig. 5) but exhibited no evidence of recrystallized melt either as a surface layer or as microscopic droplets. In these samples, the typical growth-cone structure of the pyrolytic graphite remained unaltered right up to the surface of the crater indicating that the carbon had not gone through a liquid phase transformation. It was therefore concluded that samples which contained no droplets had not melted. This conclusion is also supported by the observation that the presence as well as the size of the droplets are reproducible to within a few atmospheres of the minimum melt pressure.

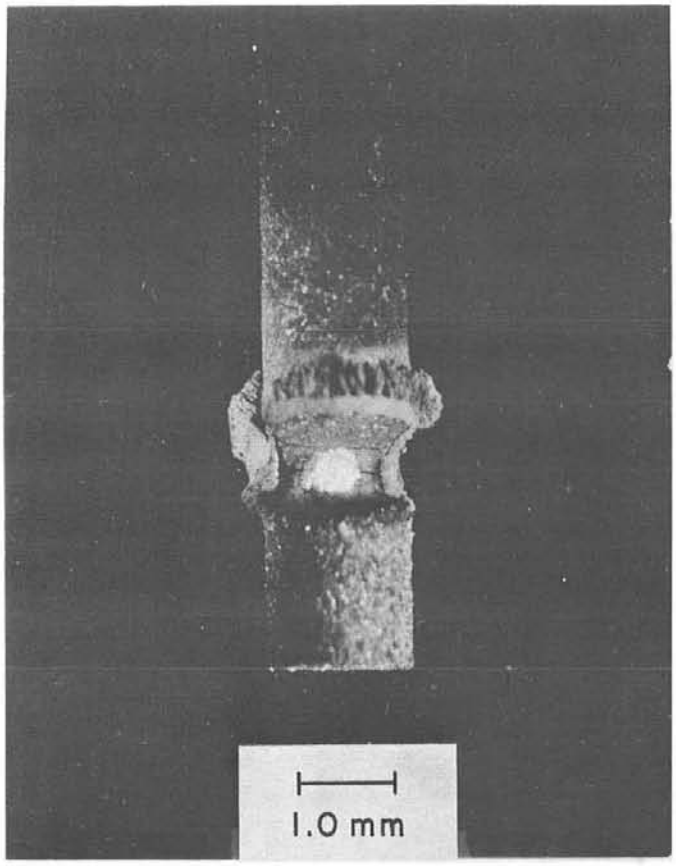

Figure 3. Laser cratered rod of pyrolytic graphite showing droplet of recrystallized melt at the bottom of the crater (147 atm Ar).

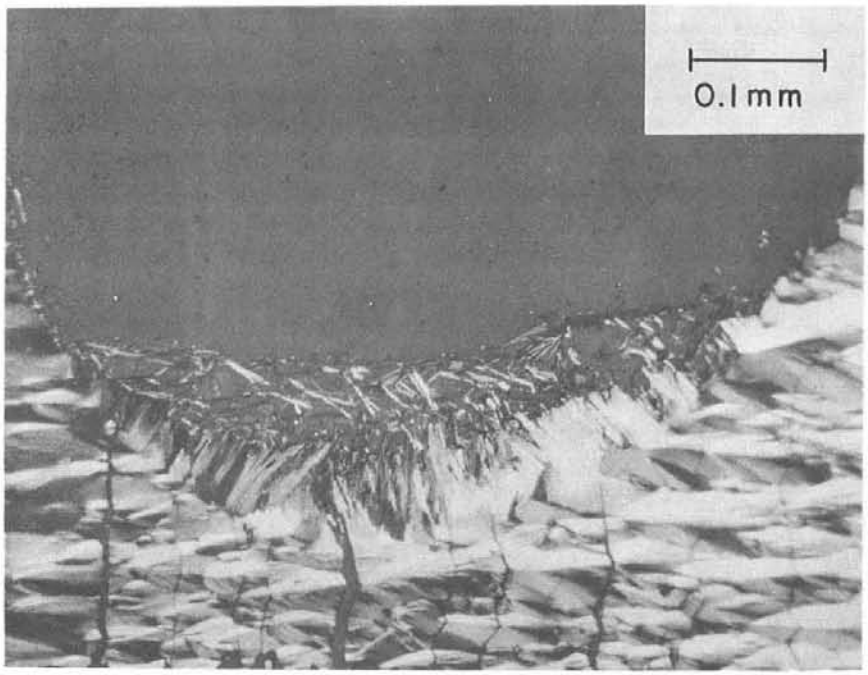

Figure 4. Microstructure of recrystallized melt at the bottom of the crater. The growth cones of the original pyrolytic graphite are evident underneath the droplet (147 atm Ar).

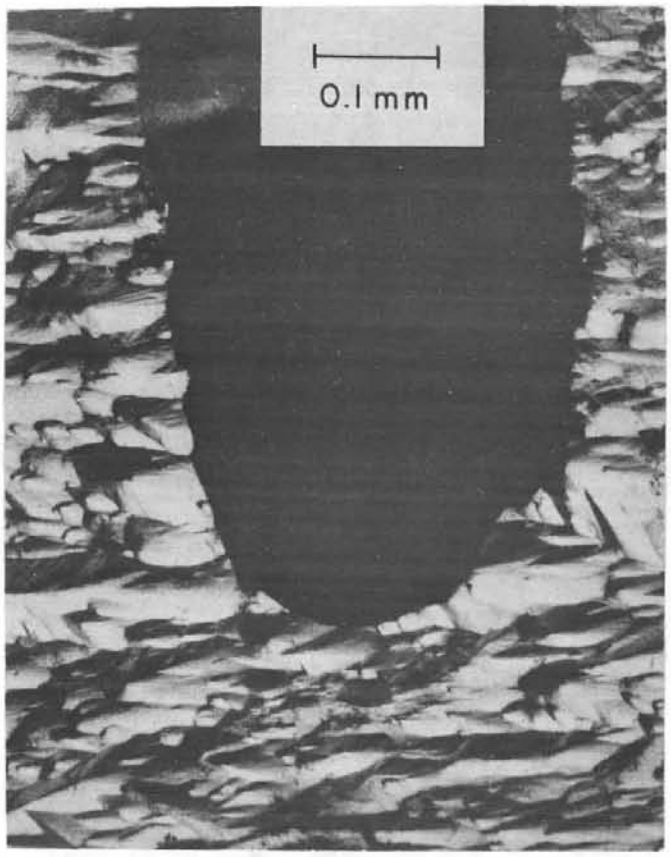

Figure 5. Microstructure of pyrolytic graphite heated with the laser at maximum power density but below the carbon triple point (105 atm Ar). Note the unaltered growth-cone structure continuing to the surface of the crater.

Additional confirmation that the droplets are recrystallized melt rather than vapor deposited material is supplied by the x-ray powder diffraction patterns obtained from the droplets. The recrystallized melt showed considerable sharpening of the diffraction lines as compared to both the original material and the vapor deposits demonstrating that the melt recrystallized into large, ordered crystallites. Representative diffraction patterns of the original carbon, vapor deposit around the crater, and recrystallized melt are given in Fig. 6. The powder diffraction patterns of natural graphite and stress-annealed pyrolytic graphite were also obtained. These two powder patterns and those of recrystallized melt were identical with respect to d-spacings. With Cu K_α radiation, indexed lines were subjected to a least-squares routine in which the lattice constants $a_o = 2.46$ Å and $c_o = 6.72$ Å were obtained. Because of the methods employed here, the difference between these values and those found by Noda[6] for recrystallized melt and natural graphite ($a_o = 2.461$ Å and $c_o = 6.708$ Å) should not be construed as being significant.

Laser Irradiation and Temperature Measurements. Several hundred carbon melting experiments were performed under a variety of experimental conditions. Initially each sample received several separate laser heatings along its length by raising or lowering the sample within the pressurized vessel. However, laser heating subsequent to the first irradiation resulted in lower measured temperatures often accompanied by larger than normal pressure excursions. It is possible that soot particles or outgassed impurities initiated a gas breakdown within the intense electric field of the focused laser beam. The resultant ionized gas in front of the sample could then absorb a portion of the laser energy and limit the amount of power delivered to the sample. This gas breakdown phenomenon has been observed often in the past,[26-30] but has generally been shown to require greater laser power densities than available here. However, high pressures,[27,28] small particles,[30] impurities[26] and hot surfaces[29] are all known to decrease the required initiation power densities. In any case, this difficulty was alleviated by limiting

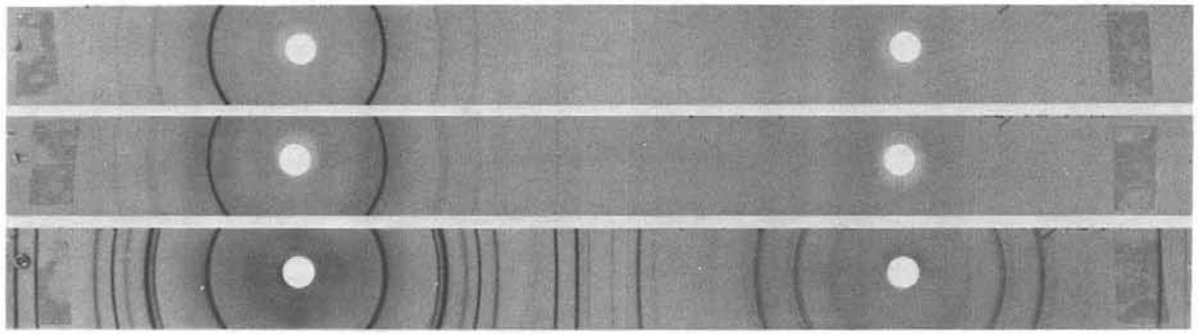

Figure 6. X-ray powder diffraction patterns of the original pyrolytic graphite samples (top), vapor deposits of carbon surrounding the crater of a laser heated sample (middle), and recrystallized melt from the bottom of the crater (bottom).

each sample to only one laser heating and implementing an efficient gas purging system before and after each experiment.

However, the pyrometrically determined temperatures still showed considerable variation ($\sim$ 4000 K to $\sim$ 5500 K), and it was concluded that the temperatures were not those strictly representative of the sample surface but rather were dominated by the dense plume in front of the graphite rod at the high pressures. This conclusion is supported by several observations. High-speed motion photography of the heating event showed that, over the wavelength sensitivity of the film, the plume obscured the surface of the samples. By photographing the event with neutral density filters spanning a thousand-fold intensity variation, it was assured that the observations were not a result of film saturation. (Films taken during laser heating at one atmosphere do, however, show that the sample surface is visible with less interference from the diffuse plume.) It was also observed that the temperatures measured in argon were consistently higher than those in helium. This would be expected of a vapor or particle plume cooled to a greater extent in helium because of the higher thermal conductivity of helium. Finally, at the instant the laser beam was turned off, the temperature often showed a very rapid decrease followed by a slow rise before finally cooling to room temperature (Fig. 7). This is most readily explained in terms of a vapor plume rapidly cooling and condensing to form a soot which effectively blocks the pyrometer's view of the sample. This soot is quickly carried out of the field of view by convection exposing the hot sample to the pyrometer. By extrapolating the slow temperature decay curve to time = 0, it was hoped that the interfering effects of the plume could be eliminated and the actual temperature of the sample estimated at the instant the laser was shut off. However, the temperature extrapolations were quite large ($\geq$ 1000 K) and exhibited significant variability. Extrapolations were very sensitive to the method of extrapolation as well. Because the dominant heat loss mechanisms and the thermal properties of carbon vary with temperature, no simple and unified functional form of the cooling curves could be relied upon as providing a basis for the extrapolations. The variability encountered and the large extrapolations required made any further analysis of the cooling curves unwarranted.

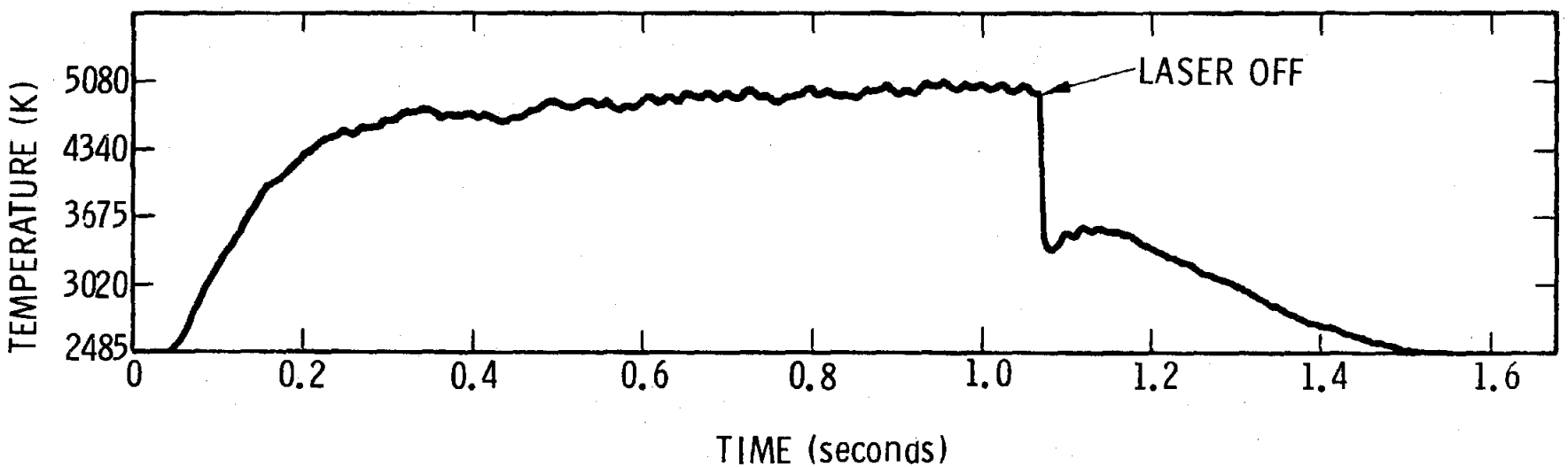

Figure 7. Representative pyrometer output as a function of time. Note that pyrometer output is non-linear with temperature and is not sensitive to temperatures much below 2500K. Temperatures are brightness temperatures corrected for fused silica windows. Sample was 1.5 mm diameter pyrolytic graphite in 147 atm argon irradiated at ~ 35 KW/cm^2.

Temperature determinations as a function of laser power and inert gas pressure resulted in inconsistent and therefore unreliable results. Temperature measurements taken along the circumference of the sample where the plume is not interfering (i.e. 90° from the laser beam) are quite low (3600 K - 3700 K) and should not be considered representative of the crater temperature. These low temperatures are probably a result of the low thermal conductivity of carbon which has been observed at high temperatures[33,34] and, therefore, only represent extreme lower limits to the actual sample temperatures.

The presence of the plume in front of the sample also prevented the direct observation of melt during the heating event. Earlier, it had been observed that because the structure of pyrolytic graphite is highly anisotropic, the emission from the edges of the basal planes is polarized in the infrared portion of the spectrum.[33] It was proposed that this property of pyrolytic graphite be used to determine the presence of the melt as it occurred by monitoring the polarization of emission from the surface of the sample. The isotropic nature of the melt would given an unpolarized emission, and therefore its presence could be detected. However, the existence of the plume prevented this direct observation.

Triple Point Pressure. The minimum pressure required for producing melt was determined as a function of sample size, laser power density, and pressurizing gas. The results are presented in Tables III and IV for the pyrolytic graphite samples. At an irradiance of $\sim$ 35 KW/cm^2, the minimum melt pressure was a function of both sample size and inert gas. This lower laser power density is therefore insufficient to completely overcome the large heat losses experienced during these experiments. Accordingly, an excessive inert gas pressure is required to reduce vaporization heat losses to a point where melting can occur. Thus the larger samples have a higher minimum melt pressure because of their greater thermal mass and larger radiative and conductive heat losses. Similar explanations are evident for the different minimum melt pressures observed in helium and argon. Samples in helium experience larger heat losses

TABLE III

RESULTS OF CARBON MELTING EXPERIMENTS

Laser Power Density ~ 35 KW/cm^2

Inert Gas	Minimum Melt Pressure	
	1.0 mm sample diameter	1.5 mm sample diameter
Argon	109 atm	111 atm
Helium	130 atm	

TABLE IV

RESULTS OF CARBON MELTING EXPERIMENTS

Laser Power Density $\sim 80\ KW/cm^2$

Inert Gas	Minimum Melt Pressure	
	1.0 mm sample diameter	1.5 mm sample diameter
Argon	107 atm	107 atm
Helium	107 atm	111 atm

due to the greater thermal conductivity of helium (see Appendix B for calculations of the relative convective heat losses in helium and argon). Samples in helium can also suffer higher vaporization heat losses due to the greater diffusion of carbon vapor through helium (see Appendix C for relative diffusion coefficients of carbon vapor in helium and argon). It is to be emphasized that these results at 35 KW/cm^2 are a direct result of insufficient laser power density.

This was confirmed by increasing the power density to ~80 KW/cm^2 (100 mm focal length lens) and observing that the minimum melt pressure of the two sample sizes (1.0 and 1.5 mm diameter) converge to 107 atmospheres (10.8 MPa). Thus, at 80 KW/cm^2 sufficient power density is delivered to overcome heat losses in each sample.

In the previous literature, the inert gas pressure associated with the minimum melt pressure has been assumed to be the carbon triple point pressure. However, for this to be the case, the pressure of carbon vapor at the surface of the sample must be identical (within experimental error) to that of the inert gas. As mentioned earlier this will be true only if the rate of vaporization exceeds the rate of transport of carbon away from the surface. Under these conditions, the partial pressure of the inert gas at the sample surface is negligible. However, if vaporization does indeed exceed the transport of carbon vapor away from the sample, then the carbon transport may be dominated by the bulk motion of carbon vapor rather than by diffusion. If this is the case, the possibility of local non-equilibrium pressure excursions exists. An estimate of these pressure excursions can be obtained from the modified Knudsen-Langmuir equation derived by Lundell and Dickey.[34] This equation relates the mass loss rate to the maximum pressure excursions.

i.e. $$p_v - p_p = \dot{m}\sqrt{2\pi RT/M_e} \qquad (1)$$

where p_v is the equilibrium vapor pressure of all carbon vapor species at temperature T, p_p is the partial pressure of the carbon vapor species at the sample surface, $\dot{m}$ is the mass loss rate of carbon per unit area, and M_e is the effective molecular weight of the carbon vapor species.

Since we are considering the case where bulk motion of the carbon vapor is sweeping all ambient inert gas species away from the carbon surface, the partial pressure of carbon vapor, p_p, at the surface is simply the static pressure of the inert gas.* Therefore $p_v - p_p$ represents the maximum pressure above ambient that can be achieved. In deriving the Eq. (1), Lundell and Dickey have assumed unit vaporization coefficients for all carbon vapor species. This should be a good approximation only if p_v-p_p is small relative to p_v. If this is the case, the high-pressure inert gas will act as a slightly porous container for the carbon vapor. Knudsen cell conditions are then approximated and vaporization coefficients should approach unity. At the maximum vaporization rates of $\sim$ 0.65 g/cm^{2}sec encountered in these experiments, the pressure excursion calculated from Eq. (1) is $<$ 0.18 atm ($<$ 0.018 MPa). Even with the vaporization coefficients reported in Ref. 13 for free vaporization conditions, the calculated pressure excursion is still only 1.4 atm (0.14 MPa) which is less than the $\pm$ 2 atm (0.2 MPa) experimental uncertainty reported here. It is therefore concluded that the overpressures encountered are not experimentally significant.

However, additional experimental data is required to ascertain the validity of the assumption that the rate of carbon vaporization exceeds the rate of vapor transport. It was accomplished by measuring the carbon minimum melt pressure in both helium and argon. As discussed earlier, the heat losses in helium are greater than in argon. In addition, the diffusion coefficient for carbon diffusing in helium is $\sim$ 3.5 times greater than that in argon (see Appendix C) while convective gas velocities are comparable in the two gases (Appendix B). Therefore the transport of carbon vapor in helium greatly exceeds that in argon. Clearly then, when laser power density is sufficient (i.e. 80 KW/cm^2), confirmation that the carbon vapor

*Strickly speaking p_p should be the stagnation pressure as calculated from Bernoulli's equation. However, at the low mass flow rates encountered in these experiments, the stagnation pressure is equal to the static pressure.

pressure is identical to the measured inert gas pressure can be made only if the minimum melt pressure of carbon is the same in both of these gases. Under these conditions, the triple point pressure of carbon can be equated with the minimum melt pressure. If the observed minimum melt pressure were not the triple point pressure, then a higher pressure would be expected in helium since its high mass diffusivity would reduce the actual partial pressure of carbon at the surface.

Experimentally it is found that the 1.0 mm diameter pyrolytic graphite sample has an identical minimum melt pressure in both helium and argon when the laser power density is adequate (80 KW/cm^2). Thus, it has been shown that the 107 ± 2 atmosphere (10.8 ± 0.2 MPa) minimum melt pressure is the triple point pressure of carbon.

It is observed that melt for the 1.5 mm diameter sample in helium is laser power limited, and the heat loses are too great to achieve melt at 107 atmospheres. A pressure of 111 atmospheres is required to melt the sample. At this higher pressure, the heat losses by vaporization have decreased sufficiently to overcome the greater heat losses of the larger sample.

The experimental data is not as clearly defined for Poco AXF-Q1 and Union Carbide SPK spectroscopic graphites. Both these polycrystalline graphites have a considerably higher thermal conductivity along the sample rod axis and a higher emissivity then the pyrolytic graphite samples used in this work.[35] Therefore the heat losses in these samples are very large and greater laser power densities are required to melt these samples at the triple point pressure. Higher laser power was not available. At the maximum power density of $\sim$ 80 KW/cm^2, a 1.0 mm diameter sample of Poco AXF-Q1 graphite required 130 (13.2 MPa) atmospheres of argon before melt could be achieved and could not be melted at all in helium to pressures as high as 165 atmospheres (16.7 MPa). Union Carbide SPK Spectroscopic grade graphite could not be melted in argon or helium to 165 atmospheres (16.7 MPa). Thus at these laser powers, there is a delicate balance of power input and output; and only with the proper thermal properties

of pyrolytic graphite could triple point data be obtained in these experiments.

Polymorphs of Carbon. In the past several years, reports of a number of new allotropes of carbon, produced by a variety of heating techniques, have appeared in the literature.[36-43] In order to assess the role of these polymorphs of carbon in the present work, samples of the recrystallized melt, vapor deposits, and graphite adjacent to the melt were examined by both x-ray and electron diffraction. No evidence of carbon polymorphs were ever seen in the x-ray diffraction patterns of any of the samples regardless of origin or temperature history. Extensive electron diffraction of the recrystallized melt did, on three isolated occasions, reveal a partial pattern corresponding to the d-spacings of previously published polymorphs. However, the d-spacings correlated only to mixtures of polymorphs and not all spots were directly identifiable as belonging to any known polymorph of carbon. Although a number of samples were extensively examined, no other evidence of these new carbon polymorphs was obtained. The limited non-graphite diffraction obtained makes it difficult to identify the few extra patterns as polymorphs of carbon or as isolated impurities. The lack of non-graphitic x-ray diffraction and limited spurious electron diffraction indicates that polymorph formation in these experiments, if present, is minor. There is no evidence, therefore, that such polymorphs play an important role in the melting of carbon under the experimental conditions described in this paper.

VI. Conclusions

The results presented in this report place the triple point pressure of carbon at 107 ± 2 atm (10.8 ± 0.2 MPa). This is in agreement with previous high pressure investigations which located the triple point of carbon between 100 and 120 atm (10 and 12 MPa). The precision of these experiments and the attention paid to detail and previous uncertainties have yielded results which tend to confirm that the preliminary low pressure carbon melt results of Whittaker et al. have been incorrectly interpreted.[16,17]

The presence of an intense vapor plume prevented accurate and direct temperature measurements at the carbon triple point. Extrapolations of cooling curves to the instant the laser was turned off eliminated the effects of this plume, but because the extrapolations were large and the data variable, no reliable temperature measurements could be obtained. The interfering effects of the plume encountered in these experiments should serve as a caution to those attempting temperature measurements in any laser heating experiments involving high vaporization rates.

The experiments presented in this report were performed to accurately define the carbon triple point pressure and to address a number of uncertainties in the previous carbon melting investigations. For the first time, accurate pressure measurements have been completed while at the same time minimizing the pressure excursions experienced during heating. Laser heating was employed rather than the traditional resistive heating, and these experiments represent the only time that data were obtained to assure that the melt pressure was not limited by power input. Finally, a set of systematic carbon melt experiments were completed in both helium and argon and maximum mass loss rates were measured to confirm the validity of the previously held assumption that the vapor pressure of carbon at the sample surface was identical to the inert gas pressure. The conclusion that must be drawn is that under equilibrium conditions pressures equalling or exceeding 107 ± 2 atm must be applied before carbon will melt.

Appendix A.

Previous Principle Investigations

Before 1939, a number of investigators[44-50] claimed to have produced liquid carbon at atmospheric pressure. In particular, Lummer's observations[44] of carbon arc electrodes in air led him to believe that he was seeing a boiling melt at the surface of the carbon anode. Later experiments conducted by Steinle[51] showed that this observation was characteristic of oxidation processes and was not present if the arc were operated in an inert atmosphere. Flow patterns and droplet appearance in deposits of resistively heated graphites also led several investigators to conclude that melt had occurred at one atmosphere. Again, Steinle[3,51] presented evidence to indicate that these observations were a result of vapor deposition and not carbon melting.

Between 1934 and 1939, Bassett[1,2] was conducting carbon melting experiments at elevated inert gas pressures using resistive heating. By 1939 he had concluded from post-heating observations of the samples that the triple point of carbon was 102 atmospheres (10.3 MPa) with a temperature $\sim$ 200 K above the carbon arc temperature (i.e. triple point temperature $\sim$ 4000 K). One year later (1940) Steinle[3] presented the results of a number of experiments up to 180 atm (18 MPa) in both argon and nitrogen. Post-heating visual examination of resistively heated samples argued that a pressure of 100 atm (10 MPa) was required before carbon could be melted. Using optical pyrometric techniques at 0.65 μm, the temperature of the melt at 100 atm was found to be 3670 K. No increase in temperature with pressure was observed. Both Bassett and Steinle found a definite sharpening of the x-ray diffraction pattern of the recrystallized melt over the original material.

In 1958, Jones[4] repeated the experiments of Bassett and Steinle and found similar results. Again post-heating observations of the samples showed a marked difference at $\sim$ 100 atm of argon pressure, and Jones assigned this pressure to the triple point of carbon. Optical pyrometry measurements at 0.65 μm indicated that his unshielded carbon rod specimens

melted at a brightness temperature of 3620 K with no detectable change in temperature between 1 and 100 atm. Results from a carbon-shielded graphite rod, drilled part way through to simulate black-body conditions, yielded a temperature rise of 220 K when the pressure was raised from 1 to 100 atm. The triple point temperature reported by Jones was 3840 K.

Noda studied the triple point of carbon initially using graphite (1959)[5] and later glassy carbon (1964).[6] The triple point pressure was found to be 110 atm (11 MPa) in both cases with the corresponding temperatures being 4020 K (graphite) and 4000 K (glassy carbon). Very few details of the experiments were presented, but it was reported that samples were heated resistively in argon and that the x-ray diffraction pattern of the resolidified melt was very similar to that of natural graphite crystals.

Between 1963 and 1968, Fateeva et al.[7-9] conducted carbon melting experiments to 60,000 atm (6000 MPa). In an argon atmosphere, resistively-melted carbon samples were monitored with 2 and 3 color pyrometers. Initial results placed the melting temperature at 4650 K with no information about triple point pressure being given. Later results placed the triple point pressure at 100 atm (10 MPa) with a corresponding temperature of 4040 K.[9] The earlier temperature measurements were labeled incorrect due to errors in filter corrections.

In 1968, G. J. Schoessow[10] conducted carbon melting experiments at elevated helium pressures using resistive heating techniques. By applying very high dc currents, Schoessow was able to heat samples large enough for a black-body cavity to be drilled in the carbon rod perpendicular to its axis. A disappearing filament pyrometer focused into this cavity was used for temperature measurement. Because gas convection currents and carbon vapor interfered with the measurements near the melt temperature, Schoessow monitored power input at temperatures below where interference was observed. By fitting power (P) and temperature to the equation $P = a_1 T^4 + a_2 T + a_3$ where T is the temperature in kelvins and a_1, a_2, and a_3 are constants, Schoessow was able to estimate the temperature of the melt from the measured power to each sample. This temperature measurement technique eliminates some but not all of the uncertainties. Although the hole drilled in the carbon samples will increase emissivity, it is not

strictly a black-body cavity due to the presence of axial temperature gradients. Also the form of the equation $P = a_1 T^4 + a_2 T + a_3$ does not specifically account for heat losses due to vaporization which are significant at the high temperatures involved. Post-heating examination of the samples was again used to confirm melt, and Schoessow reports a triple point pressure of 103 atm (10.4 MPa). The corresponding temperatures ranged from 4180 to 4300 K depending on the type of graphite melted.

In 1971, Diaconis et al.[11] reported results of both radiant arc and resistive heating of carbon samples in argon and nitrogen atmospheres. The emission from the sample was rapidly scanned from 1.4 to 3.0 μm and 2.5 - 4.4 μm, and temperatures were calculated using the results at 8 to 21 separate wavelengths. Post-heating analysis of the samples was the most extensive to data. Scanning electron micrographs and detailed microstructure of the recrystallized melt were obtained for a large number of samples. A loose, random orientation of graphite crystallites was observed whenever melt was achieved. The triple point temperature was found to range between 4100-4300 K depending on method of heating and sample type (polycrystalline ATJ-S graphite or pyrolytic graphite). These temperatures have been corrected for emissivity ($\epsilon = 0.7$ for pyrolytic graphite and $\epsilon = 0.89$ for ATJ-S). However, there is some evidence that polycrystalline graphite emissivities may be close to unity at the carbon arc temperature (3806 K).[21-22] The temperatures reported earlier in this Appendix have been brightness temperatures not corrected for emissivity.

Diaconis et al. could not determine the triple point pressure with the radiant arc heater because the plasma arc could not be operated with sufficient power below 135 atm (137 MPa). From the results of experiments using resistive heating techniques, they assign 102 atm (10.3 MPa) to the triple point pressure, but no information is given about pressure measurement techniques nor the pressure rise experienced during their ½ to 3 min. heating times.

In a very recent report, Gocken et al.[12] present results of the melting of carbon with an HF chemical laser. Neon, argon, and krypton gases were used to pressurize the system and carbon triple point values obtained were 120 atm (12 MPa) and 4130 K. Visual examination of the sample and micro-

structure analysis after heating were used to decide if melting had occurred and a disappearing filament pyrometer used for temperature measurement.

Recently Whittaker and Nelson[16] reported the results of CO_2 laser heated graphite using spinning graphite rods. Temperatures were measured with a fast response Ircon pyrometer and sample heating monitored with high-speed color photography. The collection of dimpled carbon spheres as well as the observations of high-speed color films led these authors to conclude that the triple point pressure of carbon was less than 0.25 atm (0.025 MPa). Later work[17] revealed a small cusp in the vapor pressure curve of carbon at 0.19 atm (0.019 MPa) and 3780 K. Whittaker and Kintner[17] attributed the presence of this discontinuity to the triple point of carbon. These results, however, are subject to alternate interpretation and conclusions. The results presented in this report should dispel any further belief that carbon melts below 100 atm under equilibrium conditions.

Appendix B.

Relative Convective Heat Losses in Argon and Helium

The heat losses by free convection can be compared for both helium and argon gases by standard methods.[52] The heat losses can be approximated and compared in the two gases by approximating the vertical rod as a vertical plate and using the properties of the gases at a temperature intermediate to ambient and the graphite normal sublimation temperature.

The Grashof number Gr_x for an ideal gas is then given as[52]

$$Gr_x = \frac{P^2 \, g \, x^3 \, (T_o - T_\infty) \, (MW)^2}{\mu^2 \, R^2 \, T^2}$$

The Prandtl number Pr is[52]

$$Pr = \frac{\mu \, C_P}{k}$$

and the Nusselt number Nu_x is given by

$$Nu_x = 0.508 \, Pr^{\frac{1}{2}} \, (0.952 + Pr)^{-\frac{1}{4}} \, (Gr_x)^{\frac{1}{4}}$$

where P is the pressure (taken here to be 100 atm or 1.01×10^8 dyne/cm)

g is the force of gravity

R is the ideal gas constant

MW is the molecular weight of the gas

$T_o - T_\infty$ is the difference between ambient and maximum temperature (~ 4000 K)

T is the average temperature

k is the thermal conducitivity of the gases

μ is the gas viscosity

C_p is the heat capacity at constant pressure

and x is the vertical distance from the heated portion of the sample.

Convective heat losses are then calculated from the film heat transfer coefficient (h) which is given as

$$h = \frac{Nu_x \, k}{x}$$

The specific heat flow (q) from the surface in each gas is then calculated from

$$q = h \, (T_o - T_\infty)$$

If the properties of the gases at 2000 K are used, then the following values are calculated for argon and helium:

$Pr\ (Ar) = 0.610$

$Gr_x\ (Ar) = 1.76 \times 10^6\ (x^3)$

$Nu_x\ (Ar) = 12.9\ (x^{3/4})$

$Pr\ (He) = 0.535$

$Gr_x\ (He) = 2.36 \times 10^4\ (x^3)$

$Nu_x\ (He) = 4.17\ (x^{3/4})$

For any vertical distance up the sample, the relative heat losses in helium and argon are:

$$\frac{q\ (He)}{q\ (Ar)} = \frac{Nu_x\ (He)\ k\ (He)}{Nu_x\ (He)\ k\ (Ar)} = 2.91$$

The maximum convective velocity u_{max} is given by[52]

$$u_{max} = 0.766\ (0.952 + Pr)^{-\frac{1}{2}} \left[\frac{g\ (T_o - T_\infty)}{T}\right]^{\frac{1}{2}} x^{\frac{1}{2}}$$

For a given set of conditions then the relative maximum velocity in helium and argon is only dependent on the Prandtl number and is found to be

$$\frac{u_{max}\ (He)}{u_{max}\ (Ar)} = 1.024$$

Therefore the normal free convective heat losses in helium are almost three times that in argon due predominantly to the greater thermal conductivity of helium. On the other hand, the maximum convective velocity is only a few percent greater in helium than argon.

Appendix C.

Mass Diffusivity of Carbon Vapor in Helium and Argon.

The mass diffusivity for binary mixtures of real gases is given below:[53]

$$D_{ab} = \frac{2.628 \times 10^{-19} \sqrt{(T^3)\ (\frac{1}{2})\ (\frac{1}{M_a} + \frac{1}{M_b})}}{P\ \sigma_{ab}^{\ 2}\ \Omega_2}$$

where D_{ab} = mass diffusivity, sq cm/sec

M_a = molecular weight of species a

M_b = molecular weight of species b

P = total pressures, atm.

T = temperature, K

σ_{ab}, Ω_2 = Lennard-Jones constants

$\sigma_{ab} = \frac{1}{2}(\sigma_a + \sigma_b)$

where σ_a and σ_b are the collision diameters for each molecular species. Ω_2 is the collision integral which is weakly dependent on the temperature.

C_3 has been shown to be the dominant vapor species at high temperatures and is predicted to be the dominant vapor species at the triple point temperature.[14] The C_3 species can be assumed to have Lennard-Jones constants similar to those empirically measured for CO_2 which has similar bonding and collision volume as C_3. The ratio of mass diffusivities for C_3 in helium and argon can then be approximated. Using Lennard-Jones constants based on CO_2 (see Appendix D-6 of Ref. 53), the ratio of mass diffusivities is found to be

$$\frac{D_{C_3,\ He}}{D_{C_3,\ Ar}} \simeq 3.54$$

This significant difference in mass diffusivities, which is predominantly due to the large molecular weight differences between helium and argon was used to identify the experimentally measured carbon minimum melt pressure as the triple point of carbon. This could not have been readily accomplished using gases of more similar molecular weight (e.g. Ar and N_2 used in Ref. 11).

For example, the mass diffusivity ratio of C_3 in Ar and N_2 is close to unity:

$$\frac{D_{C_3,\ N_2}}{D_{C_3,\ Ar}} = 1.09$$

References

(1) J. Basset, "The Fusion of Graphite Under a Very High Pressure of Argon up to 4000 Kg/cm^2," Comptes Rendus 208, 267 (1939).

(2) J. Basset, "Fusion of Graphite Under Argon Pressure of from 1-11,500 Kg/cm^2: Determination of the Triple Point and Construction of a Provisional Equilibrium Diagram of Carbon. Part 1," J. Phys. Radium 10, 217 (1939).

(3) H. Steinle, "Melting Experiments on Carbon," Z. Angenandte Mineralogie 2, 344 (1940).

(4) M. T. Jones, "The Phase Diagram of Carbon," Report PRC-3, National Carbon Research Laboratories, Jan. 28, 1958.

(5) T. Noda, "Melting of Carbon and Crystallinity of Molten Carbon," referred to in article by Hi Mii in "High Temperature Research in Japan," Proc. of the International Symposium on High Temperature Technology, Asilomar, California 1959, p. 431.

(6) T. Noda and M. Inagaki, "The Melting of Glassy Carbon," Bull. Chem. Soc. Japan 37, 1710 (1964).

(7) N. S. Fateeva, L. F. Vereshchagin, and V. S. Kolotygin, "Optical Method for Determining the Melting Point of Graphite as a Function of Pressure to 3000 Atmospheres," Society Physics-Doklady 8, 893 (1964).

(8) N. S. Fateeva, L. F. Vereshchagin, and V. S. Kolotygin, "Optical Method for Determining Melting Points of Graphite as a Function of Pressure up to 40,000 Atmospheres," Soviety Physics-Doklady 8, 904 (1964).

(9) L. F. Vershchagin and N. S. Fateeva, "Melting Curves of Graphite, Tungsten, and Platinum up to 60 Kilobars," Soviety Physics JETP 28, 597 (1969).

(10) G. J. Schoessow, "Graphite Triple Point and Solidus-Liguidus Interface Experimentally Determined up to 1000 Atmospheres," NASA Contractor Report, NASA CR-1148 (1968)(a); and Phys. Rev. Lett. 21, 738 (1968)(b).

(11) N. S. Dianconis, E. R. Stover, J. Hook, and G. J. Catalano, "Graphite Melting Behavior," AFML-TR-71-119, July 1971.

(12) N. A. Gokcen, E. T. Chang, T. M. Poston, and D. J. Spencer, "Determination of Graphite-Liquid-Vapor Triple Point by Laser Heating," Interim Report, SAMSO-TR-76-29, January 30, 1976.

(13) H. Palmer and M. Shelef, "Vaporization of Carbon," in Chemistry and Physics of Carbon, Vol. 4, P. L. Walker, Editor, Dekker, New York (1968).

(14) H. R. Leider, O. H. Krikorian, and D. A. Young, "Thermodynamic Properties of Carbon up to the Critical Point," Carbon 11, 555 (1973).

(15) JANAF Thermochemical Tables, Thermal Research Laboratory, Dow Chemical Co., Midland, Mich. 1960-1961, and JANAF Thermochemical Tables First Addendum, Clearinghouse for Federal Scientific and Technical Information, Washington, D.C., Aug. 1966.

(16) A. G. Whittaker and L. S. Nelson, "Measurement of Carbon Vapor Pressure and Formation of Liquid Carbon at Low Pressure by Laser Heating," Presented at the 11th Biennial Conf. on Carbon, Gatlinburg, TN, June 4-8, 1973.

(17) A. G. Whittaker and P. L. Kintner, "Carbon Solid-Liquid-Vapor Triple Point and the Behavior of Superheated Liquid Carbon," Presented at the 12th Biennial Conf. on Carbon, Pittsburgh, PA, July 28-Aug. 1, 1975.

(18) F. P. Bundy, "Melting of Graphite at Very High Pressure," J. Chem. Phys. 38, 618 (1963).

(19) Stress-annealed pyrolytic graphite was obtained from R. Bacon of Union Carbide, Parma, Ohio. X-ray powder diffraction patterns were obtained on this material at Sandia Laboratories by G. T. Gay.

(20) J.L. Margrave, "Graphite Thermodynamics," unpublished work.

(21) K. Schurer, "The Spectral Emissivity of the Anode of a Carbon Arc," Appl. Opt. 7, 461 (1968).

(22) M. R. Null and W. W. Lazier, "Measurement of Reflectance and Emissivity of Graphite at Arc Temperature with a Carbon Arc Image Furnace," J. Appl. Phys. 29, 1605 (1958).

(23) J. Euler, Ann. Physik Ser. 6 11, 203 (1953).

(24) J. Abrahamson, "Graphite Sublimation Temperatures, Carbon Arcs and Crystallite Erosion," Carbon 12, 111 (1974).

(25) R. C. Lincoln and R. C. Heckman, "Negative Pulse Thermal Diffusivity Measurements of ATJ-S Graphite to 3500 K," High Temp-High Press. 7, 71 (1975).

(26) J. F. Ready, Effects of High-Power Laser Radiation, Academic Press, New York (1971).

(27) D. L. Franzen, "Continuous Laser-Sustained Plasmas," J. Appl. Phys. 44, 1727 (1973).

(28) D. L. Franzen, "CW Gas Breakdown in Argon Using 10.6 μm Laser Radiation," Appl. Phys. Lett. 21, 62 (1972).

(29) D. C. Smith and M. C. Fowler, "Ignition and Maintenance of a cw Plasma in Atmospheric Pressure Air with CO_2 Laser Radiation," Appl. Phys. Lett. 22, 500 (1973).

(30) D. C. Smith and R. T. Brown, "Aerosol-Induced Air Breakdown with CO_2 Laser Radiation," J. Appl. Phys. 46, 1146 (1975).

(31) N. S. Razor and J. D. McClelland, "Thermal Properties of Graphite, Molybdenum and Tantalum to Their Destructive Temperatures," J. Phys. Chem. Solids 15, 17 (1960).

(32) A. E. Sheindlin, I. S. Belevich, and I. G. Kozhevikov, "Enthalphy and Specific Heat of Graphite in the Temperature Range 273-3650 K," Teplofiz. Vys. Temp. 10, 997 (1972).

(33) D. M. Haaland, "Anistropy of Emittance of Pyrolytic Graphite at 10.6 μm," Carbon 12, 633 (1974).

(34) J. H. Lundell and R. R. Dickey, "Vaporization of Graphite in the Temperature Range of 4000° to 4500°K," AIAA Paper 76-166, Jan. 1976.

(35) Y. S. Touloukian and D. P. DeWitt, Thermophysical Properties of Matter, Vol. 8, p. 31, IFI/Plenium New York, N.Y. 1972.

(36) A. El Goresy and G. Donnay, "A New Allotropic Form of Carbon from the Ries Crater," Science 161, 363 (1968).

(37) A. G. Whittaker and P. L. Kintner, "Carbon: Observations on the New Allotropic Form,"Science 165, 589 (1969).

(38) G. P. Vdovykin, "A New Hexagonal Modification of Carbon in Meteorites," Geokhimiya 9, 1146 (1969).

(39) A. G. Whittaker and G. M. Wolten, "Carbon: A Suggested New Hexagonal Crystal Form," Science 178, 54 (1972).

(40) L. S. Nelson, A. G. Whittaker, B. Tooper, "The Formation of New Polymorphs of Carbon and Fluid Flow Patterns by Irradiating Solid Carbons with a CO_2 Laser," High Temp. Sci. 4, 445 (1972).

(41) V. I. Kasatochkin, M. E. Kazakov, V. V. Savranskii, A. P. Nabatnikov, and N. P. Radimov, "Synthesis of a New Allotropic Form of Carbon from Graphite," Dokl. Akad. Nauk SSSR 201, 1104 (1971).

(42) V. I. Kasatochkin, V. V. Korshak, Y. P. Kudryavtsev, A. M. Sladkov, and I. E. Sterenberg, "On Crystalline Structure of Carbyne," Carbon 11, 70 (1973).

(43) V. I. Kasatochkin, V. V. Savranskiy, B. N. Smirnov, V. M. Mel'nichenko, "Study of the Carbyne Condensed from Carbon Vapors," Dokl. Akad, Nauk SSSR 217, 796 (1974).

(44) O. Lummer, "Melting Carbon and Production of Solar Temperatures," Viewey and Sohn, Braunschweig, p. 6, 1914.

(45) S. Münch, "Liquefaction of Carbon," Z. Elektrochem. 27, 367 (1921).

(46) E. Ryschkewitsch, "The Liquefaction of Carbon," Z. Elektrochem. 27, 445 (1921).

(47) A. Thiel and F. Ritter, "Does Carbon Melt in the Heat of an Electric Arc," Z. Anorg. Chem. 132, 153 (1923).

(48) A. Hagenbach and W. P. Luthy, "Experiments to Determine the Melting Point of Carbon," Naturwissenschaften 12, 1183 (1924).

(49) H. Alterthum, "New Investigations of Carbon Melting and Vaporization," Z. Tech. Phys. 6, 540 (1925).

(50) H. Altherthum, W. Fehse, and M. Pirani, "Determination of the Melting Point of Carbon," Z. Elektrochem. 31, 313 (1925).

(51) H. Steinle, "Lummer Phenomena at Carbon Arc and Anode Crater Temperature," Z. Angew., Mineralogie 2, 28 (1939).

(52) E. R. G. Eckert and R. M. Drake, Jr., Heat and Mass Transfer, McGraw-Hill Book Co., Inc. New York, N.Y. 1959.

(53) A. S. Faust, L. A. Wenzel, C. W. Clump, L. Mans, L. B. Andersen, Principles of Unit Operations, John Wiley & Sons, Inc., New York, 1960.

ACKNOWLEDGMENTS

The author would like to acknowledge the very valuable assistance of J. M. Freese in the construction of the apparatus, the acquisition of experimental data, and for completing post-heating sample analyses. The design of the pressure vessel by L. P. Baudoin and C. J. Greenholt was vital to the success of these experiments. In addition, the following Sandia personnel gave analytical support to this project: R. B. Foster provided several Ircon pyrometer calibrations; G. T. Gay obtained all x-ray diffraction patterns; C. R. Hills conducted the electron diffraction of the samples; and J. F. Wolcott completed the emission spectroscopy for determining impurity levels in the pyrolytic graphite samples used.

DISTRIBUTION:

Prof. John Abrahamson
Chemical Engineering Dept.
University of Canterbury
Christchurch, New Zealand

Dr. Nev Gocken
Chemistry and Physics Laboratory
The Aerospace Corp.
El Segundo, CA 90345

Prof. Howard Palmer
Department of Fuel Science
Pennsylvania State University
University Park, PA 16802

Dr. Roger Bacon
Union Carbide Corp.
Parma Technical Center
Cleveland, Ohio 44130

Prof. John L. Margrave
Department of Chemistry
Rice University
Houston, TX 77001

Dr. A. Greenville Whittaker
Aerospace Corp.
El Segundo, CA 90245

1333 S. McAlees, Jr.
Attn: I. Auerbach
D. D. McBride
5000 A. Narath
Attn: J. K. Galt - 5100
E. H. Beckner - 5200
A. W. Snyder - 5400
J. H. Scott - 5700
5443 L. S. Nelson
5800 R. S. Claassen
Attn: R. G. Kepler - 5810
M. J. Davis - 5830
D. M. Schuster - 5840
5820 R. L. Schwoebel
5824 R. W. Lynch
5825 A. W. Mullendore
5825 J. M. Freese
5825 D. M. Haaland (10)
3141 C. A. Pepmueller (Actg.) (5)
8266 E. A. Aas (2)
3151 W. L. Garner for ERDA/TIC (Unlimited Release) (3)
ERDA/TIC (25)
(R. P. Campbell, 3171-1)